Ultrafast All-Optical NOR Gate Based on Intersubband and Interband Transitions

Makoto Naruse, Haruhiko Yoshida, Tetsuya Miyazaki, Fumito Kubota, and Hiroshi Ishikawa

***Abstract*—An architecture for ultrafast all-optical digital processing, particularly NOR gates, based on intersubband and interband transitions in semiconductor quantum wells is proposed. Proof-of-principle experimental results and their analysis are also shown using InGaAs–AlAsSb coupled double-quantum-well structures that allow operation at communication wavelengths.**

***Index Terms*—Intersubband transition (ISB-T), optical signal processing, ultrafast optical switch.**

I. Introduction

SIGNAL processing using ultrafast optical time-domain devices offers significant advantages to accommodate the massive amount of traffic in terabit optical networks [1]. To perform this signal processing digitally requires a complete set of complementary logical operations, and the NOR operation forms one such set. Moreover, performance monitoring, such as error detection, is possible with NOR gates [2]. All-optical NOR gates using, for instance, optical fibers [3] or semiconductor optical amplifiers (SOAs) [4] have been successfully demonstrated. However, these have disadvantages, namely, large latency due to small nonlinearity in the case of silica fibers and low operation speed due to the large carrier life-time in the case of conventional SOAs.

II. Intersubband and Interband Transitions for All-Optical Logical Operations

The intersubband transition (ISB-T) in semiconductor quantum wells, which occurs within the conduction band, is one possible mechanism enabling all-optical logic; this mechanism has some attractive features, such as ultrafast relaxation, large transition dipole moment, and widely tunable transition wavelength [5]. Also, it has been known that the ISB-T can be used simultaneously with the interband transition (IB-T) [6], [7]. For example, when the electrons provided by n-type doping in a lower conduction subband are excited to an upper subband by ISB-T resonant light, the electron density temporarily decreases, and so the IB absorption increases. Therefore, the IB-T resonant light can be modulated by the ISB-T resonant light.

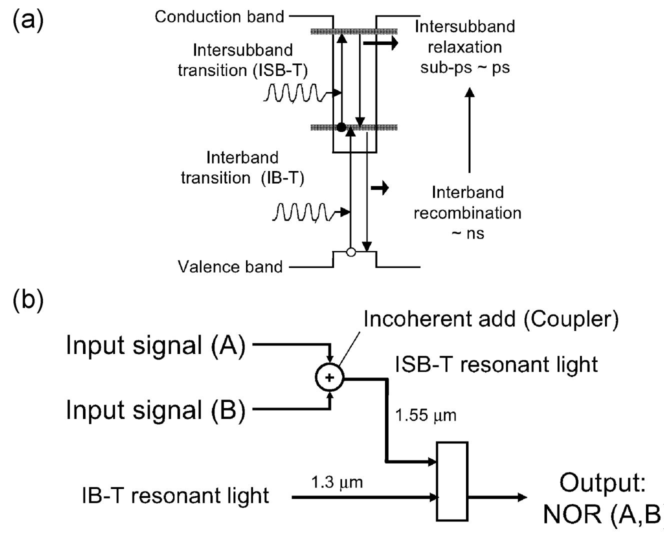

Fig. 1. (a) IB-T resonant light modulation by ISB-T resonant light. (b) Ultrafast NOR architecture using ISB-T and IB-T modulation.

In this letter, we propose applying ISB-T and IB-T to computation applications. An optical NOT gate is made possible by assigning an input signal to the ISB-T resonant light while synchronously irradiating the IB-T resonant light. The output signal is the modulated IB-T resonant light. When the input signal exists, the incident IB-T resonant light is absorbed and so the output signal does not appear. When there is no input ISB-T resonant light, the device is transparent for the IB-T resonant light and so the output signal is at the high level. Therefore, the NOT truth table is fulfilled.

Moreover, a NOR operation can also be implemented by the simple configuration shown in Fig. 1(b), where two input signals (Input A and Input B) are first added incoherently, and then act as ISB-T resonant light to the device. IB-T resonant light is also synchronously irradiated. If the pulse energy of Inputs A and B is either zero or $E_{\rm in}$, the incident energy to the device can be zero, $E_{\rm in}$, or $2 \times E_{\rm in}$. The output signal, which is the modulated IB-T resonant light, should be at the low level when the incident optical energy is both $E_{\rm in}$ and $2 \times E_{\rm in}$, thus achieving a NOR gate. This is accomplished by appropriately setting the signal level, since ISB-T causes absorption saturation. Incidentally, the number of inputs may be more than two. The NOR truth table shown in Table I shows that the output signal is one only when all inputs are zero. This NOR behavior could be applied to

Manuscript received November 29, 2004; revised March 24, 2005. This work was supported in part by the New Energy and Industrial Technology Development Organization within the framework of the Femtosecond Technology Research Project.

M. Naruse, T. Miyazaki, and F. Kubota are with National Institute of Information and Communications Technology (NICT), Koganei, Tokyo 184-8795, Japan (e-mail: naruse@nict.go.jp).

H. Yoshida was with the Femtosecond Technology Research Association (FESTA), Tsukuba, Ibaraki 300-2635, Japan. He is now with Toshiba Corporation, Kawasaki, Kanagawa 212-8582, Japan (e-mail: haruhiko.yoshida@toshiba.co.jp).

H. Ishikawa was with the Femtosecond Technology Research Association (FESTA), Tsukuba, Ibaraki 300-2635, Japan. He is now with the National Institute of Advanced Science and Technology (AIST), Tsukuba, Ibaraki 305-8568, Japan (e-mail: hiroshi-ishikawa@aist.go.jp).

Digital Object Identifier 10.1109/LPT.2005.851879

TABLE I
TRUTH TABLE OF NOR OPERATION

IN 1 (ISB-T)	IN 2 (ISB-T)	···	IN N (ISB-T)	OUT (NOR) (IB-T)
1	0	···	0	0
0	1	···	0	0
⋮	⋮	···	⋮	⋮
1	1	···	1	0
0	0	···	0	1

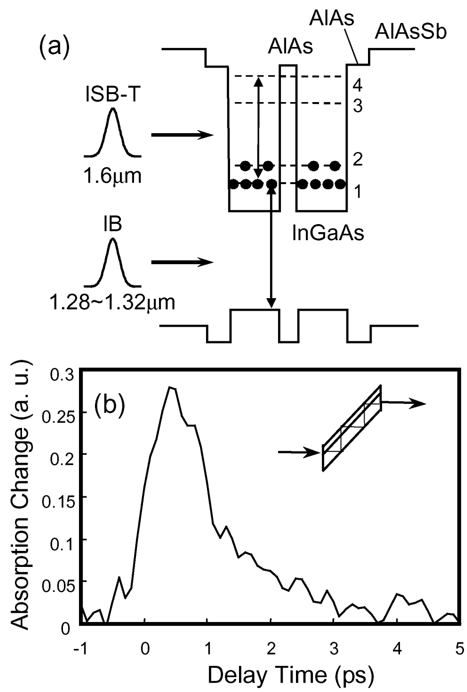

Fig. 2. (a) Band structure of the InGaAs–AlAsSb coupled double-quantum well. (b) Time evolution of the absorption change.

functionality for detecting a specific element among N distinct channels, such as to find an empty time slot for optical time-division multiplexing add–drop [8] or an empty buffer among N channels, NOR-based matching [9], and so forth.

III. EXPERIMENT USING InGaAs–AlAsSb COUPLED DOUBLE-QUANTUM-WELL (C-DQW)

Another important aspect is the operation at telecommunication wavelengths (1.3 and 1.55 μm), which is made possible by an InGaAs–AlAsSb C-DQW structure [10], shown in Fig. 2(a), where ISB-T occurs at 1.5 μm and IB-T occurs at 1.3 μm. To our knowledge, this has not been realized by other known materials. A 3.5-mm-long waveguide with 45° polished facets whose active layer was composed of a 93-period C-DQW structure was used in the experiment. The device was set in a 45° multiple reflection geometry, as shown in the inset of Fig. 2(b). An optical parametric amplifier pumped by a regenerative amplifier, which was seeded by a mode-locked Ti : sapphire laser, was used to produce 150-fs ISB-T resonant pulses (1.6 μm). IB-T resonant pulses, which covered the wavelengths ranging from 1.1 to 1.35 μm, were also generated via a sapphire plate. The IB absorption change induced by the ISB-T resonant light (Fig. 2) was integrated over the wavelength range from 1.28 to 1.32 μm; an ultrafast decay time as fast as 880 fs was achieved.

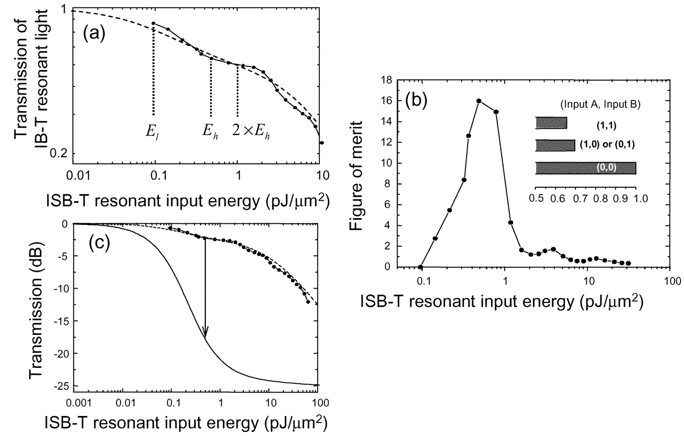

Fig. 3. (a) Transition of IB-T resonant light as a function of ISB-T input energy density. (b) FOM defined by extinction ratio, operating energy, and output level uniformity [defined in (1)]. Output signal levels at the maximum FOM (inset). (c) Expected transmission improvement by using a waveguide structure.

The transmission of the IB-T resonant light is shown in Fig. 3(a) as a function of the energy density of the incident ISB-T resonant pulses. Since our present device suffers from two-photon absorption, the absorption further increases at high input energy. For NOR logic, the transmission should be equally low for input energies of both $E_{\rm in}$ and $2 \times E_{\rm in}$ to obtain a uniform zero output level. Also, the incident ISB-T energy $E_{\rm in}$ should be as small as possible, while achieving a sufficient extinction ratio. Therefore, here we define a figure of merit (FOM) given by

$$\mathrm{FOM} = \frac{T(E_l) - T(E_h)}{E_h \times (T(2 \times E_h) - T(E_h))} \tag{1}$$

where $T(E)$ shows the IB-T transmission at incident ISB-T energy E, and E_l and E_h, respectively, represent the low and high ISB-T energies. The solid line with marks in Fig. 3(b) shows the FOM based on experimental results; it has a maximum at an ISB-T energy (E_h) of 0.49 pJ$/\mu$m^2. At this operating point, the output signal levels are summarized as shown in the inset of Fig. 3(b); that is, the NOR truth table is accomplished. The extinction ratio is, however, very small in our present device (about 2 dB); this is currently being addressed by improving the design and fabrication of the device. Further improvement is also expected by employing a ridge (or mesa) waveguide structure with relatively high optical confinement instead of the 45° multiple reflection geometry, to increase the modulation efficiency. We evaluate the transmission efficiency by introducing the following simultaneous differential equations, taking account of the guided wave structure as well as the two-photon absorption:

$$\frac{dI_{\rm ISBT}(z)}{dz} = -\left(\frac{\Gamma\alpha_{\rm ISBT} \cdot I_{sat}}{I_{\rm ISBT}(z) + I_{sat}} + \beta \cdot I_{\rm ISBT}(z)\right) \cdot I_{\rm ISBT}(z) \tag{2}$$

$$\frac{dI_{\rm IBT}(z)}{dz} = -\left(\frac{\Gamma\alpha_{\rm IBT} \cdot I_{\rm ISBT}(z)}{I_{\rm ISBT}(z) + I_{sat}} + \beta \cdot I_{\rm ISBT}(z)\right) \cdot I_{\rm IBT}(z) \tag{3}$$

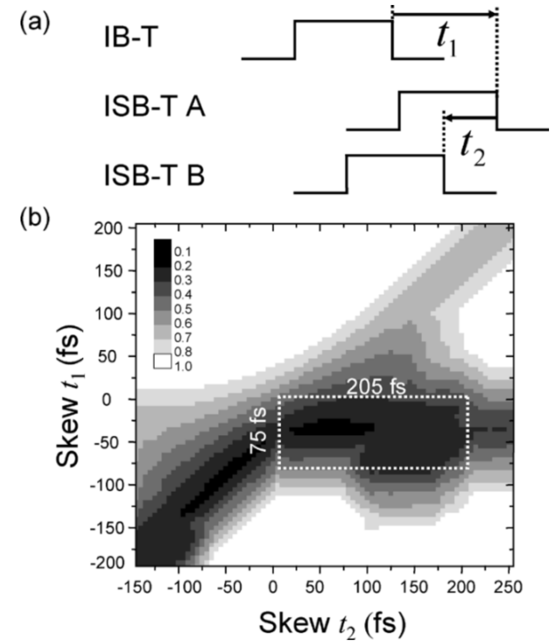

Fig. 4. (a) Skew between IB-T input and ISB-T inputs (t_1) and among ISB-T inputs (t_2). (b) Simulated output signal level as a function of t_1 and t_2.

where $I(z)$ represents the power density at the position z along the waveguide, I_{sat} is the absorption saturation power density, α and β, respectively, represent the absorption and two-photon absorption coefficients, and Γ is the light confinement factor. The subscripts ISBT and IBT on I and α indicate ISB-T and IB-T resonant light, respectively. Here, we assume a power density defined as the pulse-energy density divided by a pulse duration of 130 fs. The dashed curves in Fig. 3(a) and (c) represent fitted curves derived from the above model, which agree well with the experimental results. With a 200-μm-long waveguide, the IB-T transmission, which is given by $I_{\rm IBT}(200\,\mu{\rm m})/I_{\rm IBT}(0)$, may be improved by as much as 15 dB at an ISB-T input energy density of 0.49 pJ/μm^2, as shown in Fig. 3(c), and its corresponding FOM will improve by as much as 25.

As usual with the case of ultrafast optical switches, the skew requirements are relatively strict. There are two types of skew with a two-input system: 1) the skew between ISB-T and IB-T resonant signals, and 2) the skew between the ISB-T signals themselves; these are schematically shown in Fig. 4(a) as t_1 and t_2, respectively. Here we discuss the acceptable amount of skew based on a simple model when two inputs are at level one (high). The transmission change for IB-T light is modeled by a convolution of the incident ISB-T light profile and the impulse response of the device. The ISB-T resonant light incident on the device is modeled by the addition of a rectangular pulse of width 100 fs. The impulse response of the device is modeled by $\exp(-t/880\ {\rm fs})$ based on the experimental results shown in Fig. 2(b). The IB-T output level is then considered as the time-integral of the product of the IB-T resonant inputs, which are also 100-fs rectangular pulses, and the induced transmission of the device. Fig. 4(b) shows the output level as a function of t_1 and t_2. The tolerable margin, which is defined by the duration where the normalized output level is less than 0.5, is approximately 75 fs for t_1 and 205 fs for t_2. For such strict timing management, channel-monitoring mechanisms will be indispensable [11]. In addition, the NOR configuration described above is applicable to functions such as skew detection.

IV. Conclusion and Discussion

In summary, an architecture for ultrafast all-optical digital processing, particularly NOR gates, based on ISB-T and IB-T in semiconductor quantum wells has been proposed. Proof-of-principle experimental results and their analysis are also shown using InGaAs–AlAsSb C-DQW structures that allow operation at communication wavelengths. For future work, it is important to lower the switching energy from the present level; for instance, efforts toward optimizing the devices were discussed in [12]. Also, the overall physical system size will be of importance since the diffraction limit of light is much larger than that of very large scale integration (VLSI) circuits. We will also investigate function partitioning among ultrafast optics, VLSI circuits, and diffraction-limit-free nanophotonic devices [13] in terms of operating speed, size, and functional complexity.

References

[1] S. A. Hamilton, B. S. Robinson, T. E. Murphy, S. J. Savage, and E. P. Ippen, "100 Gb/s optical time-division multiplexed networks," *J. Lightw. Technol.*, vol. 20, no. 12, pp. 2086–2100, Dec. 2002.
[2] L. Y. Chan, K. K. Qureshi, P. K. A. Wai, B. Moses, L. F. K. Lui, H. Y. Tam, and M. S. Demokan, "All-optical bit-error monitoring system using cascaded inverted wavelength converter and optical NOR gate," *IEEE Photon. Technol. Lett.*, vol. 15, no. 4, pp. 593–595, Apr. 2003.
[3] M. N. Islam, "All-optical cascadable NOR gate with gain," *Opt. Lett.*, vol. 15, pp. 417–419, 1990.
[4] A. Sharaiha, H. W. Li, F. Marchese, and J. Le Bihan, "All-optical logic NOR gate using a semiconductor laser amplifier," *Electron. Lett.*, vol. 33, pp. 323–325, 1997.
[5] E. Rosencher, B. Vinter, and B. Levine, Eds., *Intersubband Transitions in Quantum Wells*. New York: Plenum, 1991.
[6] S. Noda, T. Uemura, T. Yamashita, and A. Sasaki, "Analysis on interband-resonant light modulation by intersubband-resonant light in n-doped quantum wells," *IEEE J. Quantum Electron.*, vol. 28, no. 2, pp. 493–500, Feb. 1992.
[7] A. Neogi, "Transient interband light modulation via intersubband coupling light in undoped semiconductor quantum wells," *Opt. Commun.*, vol. 133, pp. 479–486, 1997.
[8] S. Diez, R. Ludwig, and H. G. Weber, "Gain-transparent SOA-switch for high-bitrate OTDM add/drop multiplexing," *IEEE Photon. Technol. Lett.*, vol. 11, no. 1, pp. 60–62, Jan. 1999.
[9] H. Miyatake, M. Tanaka, and Y. Mori, "A design for high-speed low-power CMOS fully parallel content-addressable memory macros," *IEEE J. Solid-State Circuits*, vol. 36, no. 6, pp. 956–968, Jun. 2001.
[10] H. Yoshida, T. Simoyama, A. V. Gopal, J. Kasai, T. Mozome, and H. Ishikawa, "Ultrafast all-optical switching and modulation using intersubband transitions in coupled quantum well structures," *IEICE Trans. Electron.*, vol. E87-C, pp. 1134–1141, 2004.
[11] M. Naruse, H. Mitsu, M. Furuki, I. Iwasa, Y. Sato, S. Tatsuura, and M. Tian, "Femtosecond timing measurement and control using ultrafast organic thin films," *Appl. Phys Lett.*, vol. 83, pp. 4869–4871, 2003.
[12] S. Sekiguchi, T. Simoyama, H. Yoshida, J. Kasai, T. Mozume, and H. Ishikawa, "Waveguide design of InGaAs/AlAs/AlAsSb Inter-subband transition optical switch," in *Optical Fiber Communication Conf. [CD-ROM]*, Washington, DC, 2005, Paper OFE4.
[13] M. Ohtsu, K. Kobayashi, T. Kawazoe, S. Sangu, and T. Yatsui, "Nanophotonics: Design, fabrication, and operation of nanometric devices using optical near fields," *IEEE J. Sel. Topics Quantum Electron.*, vol. 8, no. 4, pp. 839–862, Jul./Aug. 2002.